

## Quantum metrology with cold atomic ensembles

Morgan W. Mitchell<sup>1,2,a</sup>, R. J. Sewell<sup>1</sup>, M. Napolitano<sup>1</sup>, M. Koschorreck<sup>3</sup>,  
B. Dubost<sup>1,4</sup>, N. Behbood<sup>1</sup> and M. Kubasik<sup>5</sup>

<sup>1</sup>*ICFO-Institut de Ciències Fòniques, Mediterranean Technology Park, 08860 Castelldefels (Barcelona), Spain*

<sup>2</sup>*ICREA – Institució Catalana de Recerca i Estudis Avançats*

<sup>3</sup>*Cavendish Laboratory, University of Cambridge, JJ Thompson Avenue, Cambridge CB3 0HE, UK*

<sup>4</sup>*Univ. Paris Diderot, Sorbonne Paris Cité, Laboratoire Matériaux et Phénomènes Quantiques, UMR 7162, Bât. Condorcet, 75205 Paris Cedex 13, France*

<sup>5</sup>*Optos, Carnegie Campus, Dunfermline, KY11 8GR, Scotland, UK*

**Abstract.** Quantum metrology uses quantum features such as entanglement and squeezing to improve the sensitivity of quantum-limited measurements. Long established as a valuable technique in optical measurements such as gravitational-wave detection, quantum metrology is increasingly being applied to atomic instruments such as matter-wave interferometers, atomic clocks, and atomic magnetometers. Several of these new applications involve dual optical/atomic quantum systems, presenting both new challenges and new opportunities.

Here we describe an optical magnetometry system that achieves both shot-noise-limited and projection-noise-limited performance, allowing study of optical magnetometry in a fully-quantum regime [1]. By near-resonant Faraday rotation probing, we demonstrate measurement-based spin squeezing in a magnetically-sensitive atomic ensemble [2–4]. The versatility of this system allows us also to design metrologically-relevant optical nonlinearities, and to perform quantum-noise-limited measurements with interacting photons. As a first interaction-based measurement [5], we implement a non-linear metrology scheme proposed by Boixo et al. with the surprising feature of precision scaling better than the  $1/N$  “Heisenberg limit” [6].

### 1. INTRODUCTION

The ability to measure magnetic fields with high sensitivity is a key requirement in many physical, biological and medical applications. Examples can be found in the measurement of geomagnetic anomalies, magnetic fields in space as well as the measurement of biomagnetic fields such as the mapping of electric and magnetic fields produced in the brain [7–9].

Optical magnetometers, based on optical readout of magnetic atomic ensembles, are currently the most sensitive instruments for measuring low-frequency magnetic fields. These instruments have demonstrated sensitivities better than  $1 \text{ fT}/\sqrt{\text{Hz}}$ , with rapid advancement in recent years [10–13]. Two distinct sources of quantum noise determine the fundamental sensitivity of this technique: the atomic projection noise and the optical polarization noise, a manifestation of shot noise [2, 14–16]. As today’s most advanced magnetometers approach the standard quantum noise limits [17] understanding these limits becomes critical for future advances [10].

---

<sup>a</sup>e-mail: [morgan.mitchell@icfo.es](mailto:morgan.mitchell@icfo.es)

For magnetometers based on Faraday rotation and optimized for sensitivity, contributions from projection noise and light-shot noise are expected to be comparable [12, 14]. A pair of techniques for reducing these fundamental noise sources have been proposed, spin squeezing of the atomic ensemble [18, 19] and polarization squeezing of the probe light [14], with potential to reduce the noise to the Heisenberg limit [16], except in the long-time regime where spin relaxation is limiting [14], see also [15]. Reduction of optical polarization noise in optical magnetometers has been demonstrated [20, 21] and recent experiments using optical quantum non-demolition (QND) measurements have demonstrated spin squeezing [17, 22–24], but thus far only with real or effective spin-1/2 systems, and with magnetically-insensitive atoms, for example squeezing of clock transitions in alkali atoms.

Here we report spin squeezing in a large-spin ( $f > 1/2$ ) atomic ensemble via QND measurement, following the strategy pioneered by Kuzmich and co-workers [19]. We pay careful attention to calibrating the spin-noise in our measurement [2], and controlling noise introduced from non-polarization spin variables [3], which have proven challenging in large-spin systems [25]. We observe a conditional spin noise reduction of  $-3.2$  dB compared to the initial coherent spin state (CSS), and infer  $-2.0$  dB of metrologically significant spin squeezing.

## 2. OPTICAL QND OF LARGE-SPIN ATOMS

We work with an ensemble of  $f = 1$  atoms interacting with pulses of near-resonant polarized light. As described in references [26, 27], the light and atoms interact by the effective Hamiltonian  $\hat{H}_{\text{eff}}$

$$\tau \hat{H}_{\text{eff}} = G_1 \hat{S}_z \hat{J}_z + G_2 (\hat{S}_x \hat{J}_x + \hat{S}_y \hat{J}_y), \quad (1)$$

where  $\tau$  is the duration of the pulse and  $G_{1,2}$  are coupling constants that depend on the beam geometry, excited-state linewidth, laser detuning, and the hyperfine structure of the atom. The atomic variables  $\hat{\mathbf{J}}$  are collective spin operators  $\hat{J}_k \equiv \sum_i^{N_A} \hat{J}_k^{(i)}$  where the superscript indicates the  $i$ -th atom and  $\hat{j}_x \equiv (\hat{j}_x^2 - \hat{j}_y^2)/2$ ,  $\hat{j}_y \equiv (\hat{j}_x \hat{j}_y + \hat{j}_y \hat{j}_x)/2$  and  $\hat{j}_z \equiv \hat{j}_z/2$ . For  $f = 1$ , these obey commutation relations  $[\hat{j}_x, \hat{j}_y] = i \hat{j}_z$  and cyclic permutations. The light is described by the Stokes operators  $\hat{S}$  defined as  $\hat{S}_\alpha \equiv \frac{1}{2}(\hat{a}_+^\dagger, \hat{a}_-^\dagger) \sigma_\alpha (\hat{a}_+, \hat{a}_-)^T$ , where the  $\sigma_\alpha$  are the Pauli matrices and  $\hat{a}_\pm$  are annihilation operators for the temporal mode of the pulse and circular plus/minus polarization.

The  $G_1$  term in Eq. (1) describes a QND interaction (paramagnetic Faraday rotation) while the  $G_2$  term describes a rank-2 tensorial atom-light coupling. For spin-1/2 atoms the  $G_2$  term vanishes identically and Eq. 1 describes a pure QND measurement. However, for  $f \geq 1$  atoms the  $G_2$  term spoils the QND interaction even in the large-detuning limit [3, 28]. To recover the ideal QND interaction, we use a two-polarization probing technique based on dynamical decoupling methods, described in detail in Ref. [3]. Briefly, we use a composite pulse sequence of alternating orthogonal polarizations of light,  $\langle \hat{S}_x^{(v)} \rangle = -\langle \hat{S}_x^{(h)} \rangle = N_L/2$ , such that, for an input  $\hat{J}_x$ -aligned CSS, the effect of the  $G_2$  term is cancelled to first order. For weak pulses, i.e.  $\langle \hat{S}_x \rangle$  sufficiently small, the system variable  $\hat{J}_z$  and meter variable  $\hat{S}_y$  after the two pulses are

$$\begin{aligned} \hat{J}_z^{(\text{out})} &= \hat{J}_z^{(\text{in})} \\ \hat{S}_y^{(\text{out})} &= \hat{S}_y^{(\text{in})} + 2G_1 \hat{S}_x^{(\text{in})} \hat{J}_z^{(\text{in})}, \end{aligned}$$

where  $\hat{S}_y' \equiv \hat{S}_y^{(v)} - \hat{S}_y^{(h)}$ .

We define a normalized measurement variable  $\hat{\phi} \equiv \hat{S}_y^{(\text{out})}/2G_1 \hat{S}_x^{(\text{in})}$ , corresponding to the scaled rotation angle of the input light polarization, so that  $\hat{\phi} = \hat{\phi}_n + \hat{J}_z^{(\text{in})}$ , where  $\hat{\phi}_n$  contains the electronic and light noise contributions to the measurement. A projection-noise limited measurement of  $\hat{J}_z$  leads to a conditionally spin squeezed state. The quantum noise reduction can be estimated from two successive measurements of  $\hat{\phi}$ : the outcome,  $\phi_1$ , of the first measurement allows us to predict the outcome,  $\phi_2$ , of a successive measurement with an accuracy given by the measurement uncertainty. The best estimate

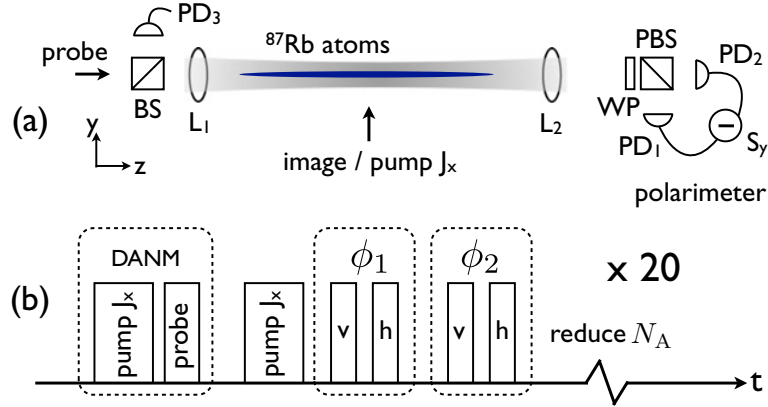


**Figure 1.** (a) Experimental geometry. PD: photodiode; L: lens; WP: waveplate; BS: beam-splitter; PBS: polarizing beam-splitter. (b) Measurement pulse sequence. See text for details.

for  $\phi_2$  is  $\chi\phi_1$ , where  $\chi = \text{cov}(\phi_1, \phi_2)/\text{var}(\phi_1)$  is the correlation between the two measurements. The conditional variance,  $\text{var}(\hat{J}_z|\phi_1) \equiv \text{var}(\phi_2 - \chi\phi_1)$ , then quantifies the noise reduction [29].

## 2.1 Experiment

We use the two-polarization probing technique to perform a QND measurement on an ensemble of up to  $8.4 \times 10^5$  laser cooled  $^{87}\text{Rb}$  atoms in the  $f = 1$  ground state. In the atomic ensemble system, illustrated in Fig. 1(a) and described in detail in Ref. [30],  $\mu\text{s}$  pulses interact with an elongated atomic cloud held in an optical dipole trap and are detected by a shot-noise-limited polarimeter. The trap geometry produces a large atom-light interaction for light propagating along the trap axis. In earlier experiments we have measured an effective on-resonance optical depth  $d_0 > 50$ . The experiment achieves projection-noise-limited sensitivity, as calibrated against a thermal spin state [2].

The measurement sequence is illustrated in Fig. 1(b). For each measurement we prepare a  $\hat{J}_x$ -aligned coherent spin state via optical pumping and measure  $N_A$  via dispersive atom number measurement (DANM) [3]. We then re-prepare the CSS and make two successive QND measurements to first prepare a conditional spin squeezed state and then verify the noise reduction. We vary  $N_A$  from  $4 \times 10^4$  to  $8.4 \times 10^5$  by briefly switching off the optical dipole trap for  $100 \mu\text{s}$  after each measurement, which reduced the atom number by  $\sim 15\%$ , and repeating the sequence 20 times per trap loading cycle. At the end of each cycle the measurement is repeated once without atoms in the trap to measure the statistics of  $\hat{\phi}_n$ . To collect statistics, the entire cycle is repeated  $\sim 10^3$  times.

For the DANM measurement we prepare the CSS and stabilize the atomic alignment with a weak magnetic field  $B_x = 10 \mu\text{T}$ . We then send pulses of circularly polarized light,  $\langle \hat{S}_z \rangle = N_L/2$ , through the cloud at a detuning of 190 MHz to the red of the  $5S_{1/2}(f=1) \rightarrow 5P_{3/2}(f'=0)$  transition with on average  $N_L = 1.2 \times 10^6$  photons per pulse, and measure  $\langle \hat{S}_y^{\text{(out)}} \rangle = G_2 N_L N_A/4$ . The QND measurements are made by sending a train of  $2 \mu\text{s}$  long pulses of light with alternating polarization through the elongated cloud at a detuning of 600 MHz to the red of the  $5S_{1/2}(f=1) \rightarrow 5P_{3/2}(f'=0)$  transition. Each pulse has on average  $N_L = 2 \times 10^9$  photons. The  $G_{1,2}$  coupling constants for the dispersive spin measurements are calibrated in separate experiments.

## 3. SPIN SQUEEZING RESULTS

To demonstrate spin squeezing, we first verify the projection-noise scaling of the QND measurements. Figure 2 shows the individual variances of the two measurements (blue circles and black diamonds)

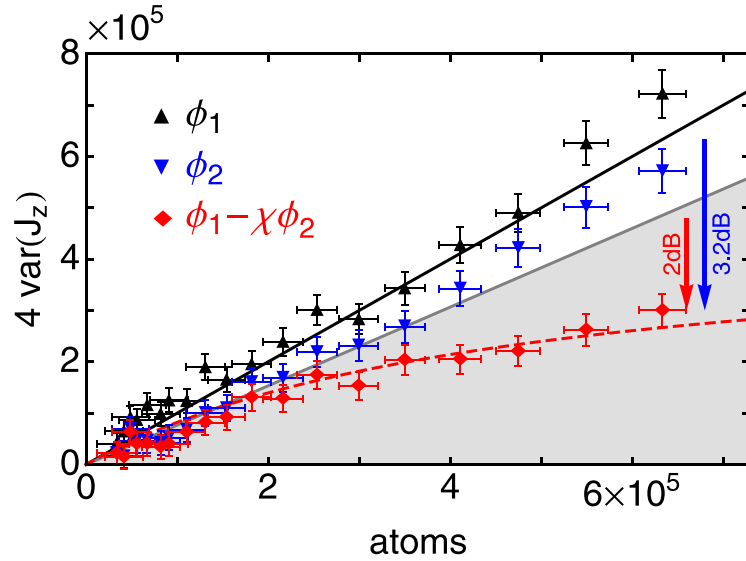


**Figure 2.** Noise scaling of the QND measurement of the CSS and spin-squeezed state. Curves are plotted from independently measured experimental parameters. The horizontal and vertical error bars are, respectively, the standard error of the variances and standard deviation of the  $N_A$  measurement. The measured read-out-noise has been subtracted from each data set.

as a function of  $N_A$ . The CSS has an expected variance  $(\Delta \hat{J}_z)_C^2 = N_A/4$  (solid black line) that scales linearly with  $N_A$ . A quadratic fit,  $4 \text{ var}(\hat{J}_z) = a_0 + a_1 N_A + a_2 N_A^2$ , to the measured data yields  $a_1 = 0.90$  and  $a_1 = 0.91$  respectively for the two measurements, consistent with the expected scaling within experimental uncertainties, and  $a_2$  coefficients consistent with zero, i.e. no observable atomic technical noise.

A nondestructive measurement of the atomic spin  $\hat{J}_z$  projects the initially prepared CSS onto a spin-squeezed state with an uncertainty equal to the measurement precision. The sensitivity of an ideal optical QND measurement is limited by the shot-noise of the probe light,  $\text{var}(\hat{S}_y) = N_L/2$ . We define a signal-to-noise ratio  $\zeta = G_1^2 N_L N_A/2$ , the ratio of the projection-noise of the CSS to the shot-noise of the light, that determines the predicted noise reduction,  $(\Delta \hat{J}_z)_S^2 = (\Delta \hat{J}_z)_C^2 / (1 + \zeta)$  [31, 32], where we calculate  $\zeta$  from independently measured experimental parameters (orange dashed line). For the maximum number of atoms used in the experiment we predict a noise reduction of  $-3.8$  dB with respect to the initial CSS. The observed noise reduction,  $\text{var}(\hat{J}_z|\phi_1)$  (orange diamonds), is slightly smaller,  $-3.2$  dB, consistent with experimental uncertainties.

To demonstrate spin squeezing, we use the Wineland criterion,  $\xi_m^2 \equiv (\Delta \hat{J}_z)_S^2 N_A / |\langle \hat{J}_x \rangle_S|^2$ , where  $\xi_m^2 < 1$  guarantees metrological advantage in using the spin-squeezed state over a CSS with equivalent polarization [33], and entanglement amongst the atoms [34]. In an atomic ensemble with finite optical depth, photon scattering during the QND measurement reduces the alignment of the CSS:  $\langle \hat{J}_x \rangle \rightarrow \langle \hat{J}_x \rangle_S = (1 - \eta) \langle \hat{J}_x \rangle$ , where  $\eta \propto G_1 N_L$  limits the achievable spin squeezing [31, 32]. For the photon number,  $N_L = 3 \times 10^9$ , used in the first QND measurement we measure  $\eta = 0.11$ . We satisfy the Wineland criterion if the conditional variance of the spin-squeezed state is less than the projection-noise of the CSS reduced by a factor  $(1 - \eta)^2$  (grey solid line in Fig. 2). For the maximum number of atoms used in the experiment we infer  $\xi_m^2 = 0.63$ , giving 2.0 dB of metrologically significant spin squeezing.

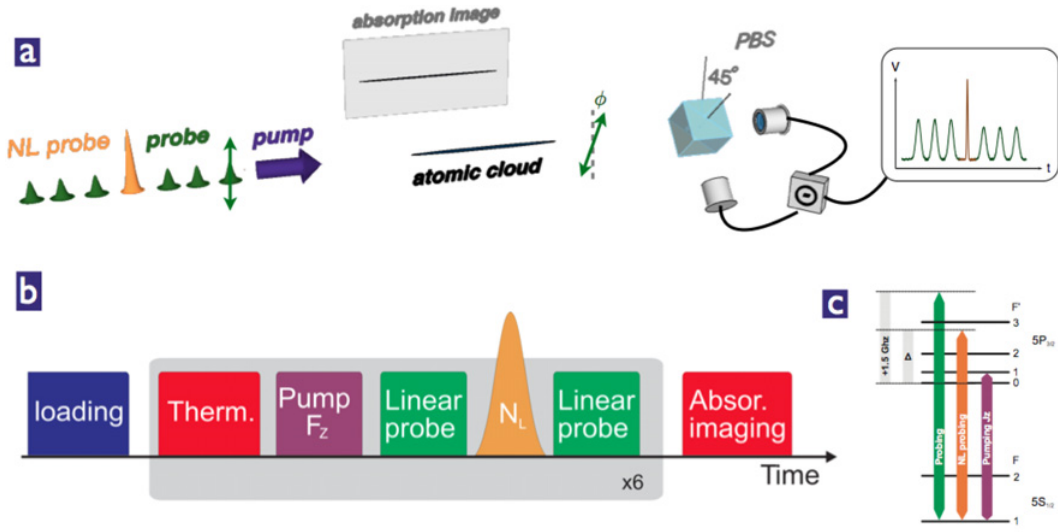


**Figure 3. Interaction-based measurement** a) Experimental schematic: an ensemble of  $(7 \times 10^5)^{87}\text{Rb}$  atoms, held in an optical dipole trap, are optically probed on axis, with the resulting Faraday rotation measured by a shot-noise-limited polarimeter (PM). b) experimental sequence: the atoms are first prepared in  $(|F = 1, m_F = 1\rangle)$  by optical pumping (Pump), then measured by Linear, Nonlinear, and a second Linear Faraday rotation probing. The atom number is measured by quantitative absorption imaging (AI). c) Spectral positions of the pumping, probing, and imaging light.

#### 4. INTERACTION-BASED MEASUREMENT OF THE COLLECTIVE SPIN OF AN ENSEMBLE

Traditional discussions of quantum metrology [35, 36] describe linear interferometers, or equivalently systems of non-interacting particles, as models for precision instruments. A number of recent works have discussed the quantum limits of systems of interacting particles [6, 37–39]. This work is particularly germane to optical magnetometry because some state-of-the-art techniques employ interactions in an essential way. For example, spin-exchange-relaxation-free (SERF) techniques [10] employ atom-atom interactions to dramatically increase coherence lifetimes, while nonlinear magneto-optic rotation (NMOR) techniques use optical nonlinearities, i.e., atom-mediated photon-photon interactions [40–43]. Here we describe a test of one of the first predictions regarding quantum noise limits in systems of interacting particles. In our system it is possible to generate a controlled and tunable interaction among the probe photons. We use this to implement a proposal [6, 38] to generate *interaction-based* measurement of the collective spin of the ensemble. Full details are given in [44].

Following the discussion in [6, 38], we consider a collection of  $N$  photons, with circular plus/minus polarisations  $|+\rangle, |-\rangle$  described by single-photon Stokes operators  $\hat{s}_\alpha = (|+\rangle, |-\rangle)\sigma_\alpha(|+\rangle, |-\rangle)^T$ , where the  $\hat{s}_\alpha, \alpha \in \{x, y, z\}$  are the Pauli matrices and  $\hat{s}_0$  is the identity. We describe the polarization of the  $i$ 'th atom by  $\hat{s}_\alpha^{(i)}$ . In linear quantum metrology, a Hamiltonian of the form

$$\hat{H}_L = \mathcal{X} \sum_{i=1}^N \hat{s}_z^{(i)} \quad (2)$$

uniformly and independently couples the photons to  $\mathcal{X}$ , the parameter to be measured [36]. If the input state consists of independent photons, the possible precision scales as  $\delta\mathcal{X} \propto N^{-1/2}$ , the shot-noise or

standard quantum limit (SQL). The  $N^{-1/2}$  factor reflects the statistical averaging of independent results. In contrast, entangled states can be more strongly correlated than non-entangled ones, giving precision limited by  $\delta\mathcal{X} \propto N^{-1}$ , known as the Heisenberg limit (HL).

Systems of interacting particles do not necessarily obey these scaling laws. This is most easily seen by considering the same system, coupled to an unknown  $\mathcal{Y}$  by a Hamiltonian of the form

$$\hat{H}_{\text{NL}} = \mathcal{Y} \sum_{i \neq j} \hat{s}_z^{(i)} \hat{s}_0^{(j)}, \quad (3)$$

where  $\hat{s}_0$  is again the identity. This describes a pairwise interaction among the photons with a coupling strength  $\mathcal{Y}$ . Using the fact that  $\hat{s}_0^{(j)}$  commutes with all other operators, we can perform the sum over  $j$  to find  $\hat{H}_{\text{NL}} = \hbar N \mathcal{Y} \sum_{i=1}^N \hat{s}_z^{(i)}$ . This has the same operator character as  $\hat{H}_L$ , with an additional factor  $N$ . A measurement of  $\mathcal{Y}$  thus has limiting sensitivities  $\delta\mathcal{Y} \propto N^{-3/2}$  for independent photons and  $\delta\mathcal{Y} \propto N^{-2}$  for entangled photons. We see that measurement of interaction strengths are not constrained by the SQL and HL scaling laws that apply to measurement of single-particle rotations. It is important to note a few points. First, these results are completely consistent with the Heisenberg uncertainty principle: the quantum noise of the state is the same, independent of whether the Hamiltonian is linear or nonlinear. In contrast, the signal, i.e. the average rotation of the state, shows a different dependence on  $N$  for estimation of  $\mathcal{X}$  versus  $\mathcal{Y}$ , and thus different scaling of the signal-to-noise ratio. Second, we note that  $\mathcal{X}$  and  $\mathcal{Y}$  are not the same kind of quantity;  $\mathcal{X}$  produces a linear optical or  $\chi^{(1)}$  effect, e.g. a circular birefringence, whereas  $\mathcal{Y}$  produces a Kerr or  $\chi^{(3)}$  effect, e.g. a cross-phase modulation. The fact that  $\delta\mathcal{Y}$  falls faster with  $N$  than does  $\delta\mathcal{X}$  is consistent with the commonplace observation that nonlinear optical effects are best measured at high intensities.

A number of systems have been proposed to observe these anomalous scaling properties, including Kerr nonlinearities [45], cold collisions in condensed atomic gases [6], Duffing nonlinearity in nano-mechanical resonators [46] and a two-pass effective nonlinearity with an atomic ensemble [47]. Topological excitations in nonlinear systems may also give advantageous scaling [48].

We use a cold atomic ensemble as a light-matter quantum interface [32] to produce quantum-noise-limited interactions and a Hamiltonian of the form  $\hat{H} = \hbar \mathcal{X} \hat{S}_0 \hat{S}_z = \hbar \mathcal{X} N \hat{S}_z$ . This Hamiltonian gives a polarization rotation growing with  $N$  without increasing quantum noise [6]. The experiment uses the same cold atomic ensemble system described earlier, but with shorter, higher-intensity probe pulses tuned closer to resonance, in order to achieve the desired nonlinear interaction. The linear optical interactions that produce parametric Faraday rotation, described by Eq. (1), result from second-order application of the electric dipole interaction between quantized fields and the atomic ensemble. When this perturbative treatment is extended to fourth order [49], we find these additional contributions to the effective Hamiltonian:

$$H_{\text{eff}}^{(4)} = \beta_J^{(0)} S_Z^2 J_0 + \beta_N^{(0)} S_Z^2 N_A + \beta^{(1)} S_0 S_Z J_Z + \beta^{(2)} S_0 (S_X J_X + S_Y J_Y), \quad (4)$$

where  $J_0$  is one-half the number of atoms in the  $m_F = \pm 1$  states, and  $N_A$  is the number of atoms in the ensemble. As described in [49], with a properly chosen detuning  $\Delta_0$  relative to the  $F = 1 \rightarrow F'$  transitions of the  $D_2$  line of  $^{87}\text{Rb}$ , it is possible to make the third term, i.e.,  $\beta^{(1)} S_0 S_Z J_Z$ , dominant over all other terms, including the linear terms of Eq. (1). This nonlinear term evidently has the form of Eq. (3), and we make the association  $\mathcal{Y} = \beta^{(1)} J_Z$ . This describes a photon-photon interaction which produces a kind of nonlinear Faraday rotation. The rotation angle  $\phi$  is proportional to both the number of photons  $N = S_0$ , and to the atomic polarization  $J_Z$ .

We are now armed with two quite different ways to estimate the collective spin  $J_Z$ : we can use a linear measurement, as in section 2, or we can use a nonlinear, *interaction-based* measurement of the same quantity. Both optical measurement strategies employ non-resonant probing, and thus preserve the spin variable being measured. This allows a direct comparison of near-simultaneous measurements made on the same ensemble, and a very direct investigation of the scaling behaviour.

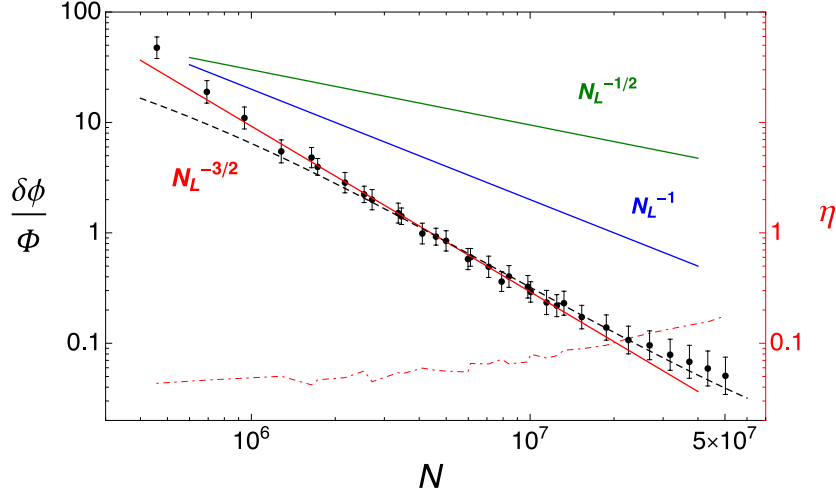


**Figure 4. Sensitivity versus size for interaction-based measurement.** Fractional sensitivity  $\delta\phi/\Phi$  of the nonlinear probe versus number of interacting photons  $N$ . Black dots indicate the measured sensitivity, black dashed curve shows results of numerical modelling, and the colored lines indicate SQL, HL, and  $N^{-3/2}$  scaling for reference. Scaling surpassing the Heisenberg limit  $\propto N_L^{-1}$  is observed over two orders of magnitude. The measured change in the atomic polarization  $\eta$ , shown as a red dashed line, confirms the non-destructive nature of the measurement.

## 5. EXPERIMENTAL TEST OF SCALING IN INTERACTION-BASED MEASUREMENT

The experimental strategy is shown in Fig. 3. The atomic ensemble is first fully polarized by optical pumping, then  $F_z$  is measured three times, once by a far-detuned, low-intensity pulse in the linear regime, then by a near-resonant high-intensity pulse, and finally a second low-intensity pulse. In each case the rotation angle is  $\langle \hat{F}_z \rangle [A(\Delta) + B(\Delta)N]/2$  where  $A \propto G_1$  and  $B \propto \beta^{(1)}$  account for the temporal pulse shape and geometric overlap between the atomic density and the spatial mode of the probe, and  $\Delta$  is the detuning from resonance. Two regimes of probing are used: the *linear probe* consists of forty  $1 \mu\text{s}$  pulses (total illumination time  $\tau_L = 40 \mu\text{s}$ ) spread over  $400 \mu\text{s}$  with detuning  $\Delta_L \gg \Delta_0$ . This gives  $A \gg N_L B$ , i.e., linear estimation. The *nonlinear probe* consists of a single  $\tau_{NL} = 54 \text{ns}$  FWHM, Gaussian-shaped, high-intensity pulse with  $N$  photons and detuning  $\Delta_0$ , so that  $A \ll NB$ . Having two probes allows us to precisely calibrate the nonlinear measurement using a highly sensitive and well characterised independent measurement of the same sample.

The noise in the nonlinear probe as a function of  $N$  is shown in Fig. 4. The sensitivity  $\delta\phi/\Phi$  vs.  $N$  where  $\Phi$  is the rotation produced by the full ensemble, i.e.,  $\hat{F}_z = 7 \times 10^5$ . In agreement with theory, the log-log slope indicates the scaling  $(\delta\phi/\Phi) \propto N^{-3/2}$  to within experimental uncertainties in the range  $N = 10^6$  to  $N = 10^7$ , and SH scaling, i.e., a slope  $< 1$ , over two orders of magnitude  $N = 5 \times 10^5$  to  $N = 5 \times 10^7$ . Also shown are the results of numerical modelling using the Maxwell-Bloch equations to describe the nonlinear light-atom interaction. The deviation at low  $N$  is consistent with a 200 kHz uncertainty in the light shift produced by the optical dipole trap.

For photon numbers above  $N \gtrsim 2 \times 10^7$ , the saturation of the nonlinear rotation alters the slope. This can be understood as optical pumping of atoms into states other than  $|F=1, m_F=1\rangle$  by the nonlinear probe. The damage to the atomic magnetisation  $\eta = 1 - \phi_L'/\phi_L$ , shown in Fig. 4 remains small, confirming the non-destructive nature of the measurement. The finite damage even for small  $N$  is possibly due to stray light and/or magnetic fields disturbing the atoms during the 20 ms period between the two linear measurements. At large  $N$ , high-order nonlinear effects including optical pumping limit the range of SH scaling.

## 6. CONCLUSIONS

We have described two quantum-limited measurements using cold atomic ensembles probed by a shot-noise-limited Faraday rotation setup. In the first, we report the first spin squeezing by quantum non-demolition measurement in a magnetically-sensitive atomic ensemble. This elusive goal was finally achieved using the combination of a high optical-depth trap geometry, dynamical decoupling of the spin alignment degrees of freedom, and a new calibration of the projection noise level based on the quantum statistics of thermal states. Spin squeezing is promising for practical application in optical magnetometry. In the second experiment, we have tested and confirmed the prediction of sensitivity scaling as  $N^{-3/2}$  when measuring the interaction strength of a system of interacting particles. By computing the nonlinear optical behaviour of the ensemble, we found a magic detuning at which the photon-photon interaction is proportional to the atomic spin polarization, allowing the first quantum-noise-limited interaction-based measurement of atomic spin. The observed sensitivities show a scaling of  $N^{-3/2}$  over more than a decade in photon number  $N$ , in agreement with simple theory and a full Maxwell-Bloch calculation. These results show that it is possible to perform quantum-noise-limited measurements with ensembles of interacting particles, and are a step toward quantum sensitivity enhancement to intrinsically nonlinear instruments such as SERF and NMOR magnetometers.

This work was funded by the Spanish MINECO under the project MAGO (Ref. FIS2011- 23520), and by the European Research Council project AQUMET.

## References

- [1] S. R. de Echaniz, M. Koschorreck, M. Napolitano, M. Kubasik, M. W. Mitchell, *Phys. Rev. A* **77**, 032316 (2008).
- [2] M. Koschorreck, M. Napolitano, B. Dubost, M. W. Mitchell, *Phys. Rev. Lett.* **104** (2010).
- [3] M. Koschorreck, M. Napolitano, B. Dubost, M. W. Mitchell, *Phys. Rev. Lett.* **105** (2010).
- [4] R. J. Sewell, M. Koschorreck, M. Napolitano, B. Dubost, N. Behbood, M. W. Mitchell, *ArXiv e-prints* (2011), 1111.6969.
- [5] M. Napolitano, M. W. Mitchell, *New J. Phys.* **12**, 093016 (2010).
- [6] S. Boixo, A. Datta, M. J. Davis, S. T. Flammia, A. Shaji, C. M. Caves, *Phys. Rev. Lett.* **101**, 040403 (2008).
- [7] W. F. Stuart, M. J. Usher, S.H. Hall, *Nature (London)* **202**, 76 (1964).
- [8] M. K. Dougherty, K. K. Khurana, F. M. Neubauer, C. T. Russell, J. Saur, J. S. Leisner, M. E. Burton, *Science* **311**, 1406 (2006).
- [9] H. Xia, A. B. Baranga, D. Hoffman, M. V. Romalis, *Appl. Phys. Lett.* **89**, 211104 (2006).
- [10] I. Kominis, T. Kornack, J. Allred, M. Romalis, *Nature* **422**, 596 (2003).
- [11] I. M. Savukov, S. J. Seltzer, M. V. Romalis, K. L. Sauer, *Phys. Rev. Lett.* **95**, 063004 (2005).
- [12] D. Budker, M. Romalis, *Nature Phys.* **3**, 227 (2007).
- [13] H. B. Dang, A. C. Maloof, M. V. Romalis, *Applied Physics Letters* **97**, 151110 (3) (2010).
- [14] M. Auzinsh, D. Budker, D. F. Kimball, S. M. Rochester, J. E. Stalnaker, A. O. Sushkov, V. V. Yashchuk, *Phys. Rev. Lett.* **93**, 173002 (2004).
- [15] I. K. Kominis, *Phys. Rev. Lett.* **100**, 073002 (2008).
- [16] V. Shah, G. Vasilakis, M. V. Romalis, *Phys. Rev. Lett.* **104**, 013601 (2010).
- [17] W. Wasilewski, K. Jensen, H. Krauter, J. J. Renema, M. V. Balabas, E. S. Polzik, *Phys. Rev. Lett.* **104**, 133601 (2010).
- [18] A. Kuzmich, K. Mølmer, E. S. Polzik, *Phys. Rev. Lett.* **79**, 4782 (1997).

- [19] A. Kuzmich, N. B. Bigelow, L. Mandel, *Europhys. Lett.* **42**, 481 (1998).
- [20] F. Wolfgramm, A. Cerè, F. A. Beduini, A. Predojević, M. Koschorreck, M. W. Mitchell, *Phys. Rev. Lett.* **105**, 053601 (2010).
- [21] T. Horrom, R. Singh, J. P. Dowling, E. E. Mikhailov, *Phys. Rev. A* **86**, 023803 (2012).
- [22] P. J. Windpassinger, D. Oblak, U. B. Hoff, A. Louchet, J. Appel, N. Kjærgaard, E. S. Polzik, *Journal of Modern Optics* **56**, 1993 (2009).
- [23] M. H. Schleier-Smith, I. D. Leroux, V. Vuletic, *Phys. Rev. Lett.* **104**, 073604 (2010).
- [24] I. D. Leroux, M. H. Schleier-Smith, V. Vuletic, *Phys. Rev. Lett.* **104**, 073602 (2010).
- [25] J. M. Geremia, J. K. Stockton, H. Mabuchi, *Phys. Rev. Lett.* **101**, 039902 (2008).
- [26] J. M. Geremia, J. K. Stockton, H. Mabuchi, *Phys. Rev. A* **73**, 042112 (2006).
- [27] S. R. de Echaniz, M.W. Mitchell, M. Kubasik, M. Koschorreck, H. Crepaz, J. Eschner, E. S. Polzik, *J. Opt. B* **7**, S548 (2005).
- [28] G. A. Smith, S. Chaudhury, A. Silberfarb, I. H. Deutsch, P. S. Jessen, *Phys. Rev. Lett.* **93**, 163602 (2004).
- [29] J. P. Poizat, J. F. Roch, P. Grangier, *Ann. Phys.-Paris* **19**, 265 (1994).
- [30] M. Kubasik, M. Koschorreck, M. Napolitano, S. R. de Echaniz, H. Crepaz, J. Eschner, E. S. Polzik, M. W. Mitchell, *Phys. Rev. A* **79** 043815 (2009).
- [31] C. Hammerer, K. Mølmer, E. S. Polzik, J. I. Cirac, *Phys. Rev. A* **70**, 044304 (2004).
- [32] K. Hammerer, A. S. Sørensen, E. S. Polzik, *Rev. Mod. Phys.* **82**, 1041 (2010).
- [33] D. J. Wineland, J. J. Bollinger, W. M. Itano, F. L. Moore, D. J. Heinzen, *Phys. Rev. A* **46**, R6797 (1992).
- [34] A. Sørensen, L. M. Duan, J. I. Cirac, P. Zoller, *Nature* **409**, 63 (2001).
- [35] V. Giovannetti, S. Lloyd, L. Maccone, *Science* **306**, 1330 (2004).
- [36] V. Giovannetti, S. Lloyd, L. Maccone, *Phys. Rev. Lett.* **96**, 010401 (2006).
- [37] A. Luis, *Phys. Lett. A* **329**, 8 (2004).
- [38] S. Boixo, S. T. Flammia, C. M. Caves, J. M. Geremia, *Phys. Rev. Lett.* **98**, 090401 (2007).
- [39] A. Luis, *Phys. Rev. A* **76**, 035801 (3) (2007).
- [40] M. W. Mitchell, C. I. Hancox, R. Y. Chiao, *Phys. Rev. A* **62**(4) (2000).
- [41] D. Budker, D. F. Kimball, S. M. Rochester, V. V. Yashchuk, M. Zolotarev, *Phys. Rev. A* **62**, 043403 (2000).
- [42] D. Budker, D. F. Kimball, S. M. Rochester, V. V. Yashchuk, *Phys. Rev. Lett.* **85**, 2088 (2000).
- [43] S. Pustelny, A. Wojciechowski, M. Gring, M. Kotyrba, J. Zachorowski, W. Gawlik, *Journal of Applied Physics* **103**, 063108 (7) (2008).
- [44] M. Napolitano, M. Koschorreck, B. Dubost, N. Behbood, R. J. Sewell, M. W. Mitchell, *Nature* **471**, 486 (2011).
- [45] J. Beltrán, A. Luis, *Phys. Rev. A* **72**, 045801 (2005).
- [46] M. J. Woolley, G. J. Milburn, C. M. Caves, *New J. Phys.* **10**, 125018 (2008).
- [47] B. A. Chase, B. Q. Baragiola, H. L. Partner, B. D. Black, J. M. Geremia, *Phys. Rev. A* **79**, 062107 (2009).
- [48] A. Negretti, C. Henkel, K. Mølmer, *Phys. Rev. A* **77**, 043606 (2008).
- [49] M. Napolitano, M. W. Mitchell, *New J. Phys.* **12**, 093016 (2010).